INSTITUTE OF PHYSICS PUBLISHING JOURNAL OF PHYSICS B: ATOMIC, MOLECULAR AND OPTICAL PHYSICS

J. Phys. B: At. Mol. Opt. Phys. **39** (2006) L241–L247 doi:10.1088/0953-4075/39/11/L03

LETTER TO THE EDITOR

Stark deceleration of hydrogen atoms

E Vliegen and F Merkt[1]

Laboratorium für Physikalische Chemie, ETH Zürich CH-8093, Switzerland

Received 6 April 2006, in final form 7 April 2006
Published 2 May 2006
Online at stacks.iop.org/JPhysB/39/L241

Abstract

Hydrogen atoms in a cold supersonic expansion with an average velocity of 700 m s^{-1} have been excited to Rydberg Stark states with principal quantum number in the range $n = 20$–25 and subsequently decelerated and accelerated in time-independent inhomogeneous electric fields. Accelerations of up to 2×10^8 m s^{-2} have been achieved and the initial kinetic energy of atoms prepared in low (high)-field seeking Stark states could be more than quadrupled (halved) over a flight distance of only 3 mm and in a time of less than 5 μs. The control over the velocity of the Rydberg atoms is such that trapping can be envisaged.

(Some figures in this article are in colour only in the electronic version)

1. Introduction

The development of general methods to produce samples of cold and ultracold atoms and molecules represents an important area of current research in physics and physical chemistry [1, 2]. When the translationally cold atoms/molecules are in high Rydberg states, one speaks of a cold Rydberg gas [3]. Studies of cold Rydberg gases have become feasible recently and are important in the contexts of quantum information processing [4, 5] and ultracold plasmas [6, 7]. Two routes can be followed to generate a cold Rydberg gas. The usual method consists of trapping ground-state atoms in a magneto-optical trap (MOT) and subsequently photoexciting them to Rydberg states [3, 8, 9]. An alternative method is to photoexcite the atoms to high Rydberg states in a cold supersonic expansion and subsequently decelerate the Rydberg atoms to close to zero velocity in the lab frame. The latter method has the advantage that it is applicable to all atoms and in principle also to molecules, and it has been shown recently to be viable although only proof-of-principle studies have been performed so far [10–16].

We report here on acceleration and deceleration experiments on H atoms excited to Rydberg states with principal quantum numbers in the range $n = 20$–25 and demonstrate that electrostatic acceleration/deceleration can be used to exert an unprecedented control on the motion of the excited atoms. For potential applications in quantum information processing

[1] Author to whom any correspondence should be addressed.

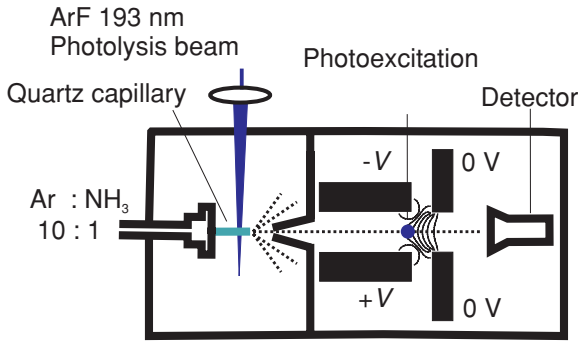

Figure 1. Schematic view of the experimental arrangement. The skimmed supersonic beam of H atoms propagates centrally through the four metallic electrodes that are used to generate an inhomogeneous field. The anticollinear UV and VUV laser beams propagate parallel to the plate surfaces and perpendicular to the atomic beam. After flying through the inhomogeneous field region, the atoms reach a microchannel plate detector where they ionize and their time of flight is registered. The solid lines are lines of constant electric field.

and studies of ultracold plasmas, hydrogen presents the important advantages of having the simplest ion core and a well-understood energy level structure. Its small mass makes it easy to manipulate, and problems associated with adiabatic traversals of the crossings between Stark states that complicate deceleration experiments in other atoms and molecules [12] are not encountered. A further reason for our efforts to accelerate, slow down, and eventually trap hydrogen atoms in Rydberg states is to establish a possible way of manipulating the velocity distribution of the antihydrogen atoms that are currently produced in high Rydberg states at CERN [17, 18].

The principle of the deceleration method can be understood as a conversion between kinetic and potential energy that takes place when a Rydberg particle moves in an inhomogeneous electric field. The experiment is thus the electric field analogue of the famous Stern–Gerlach experiment [19]. The energy levels of the H atom in an electric field F are given to first order, in atomic units, by

$$E = \frac{-1}{2n^2} + \frac{3}{2}nkF, \tag{1}$$

where k is a quantum number which runs from $-(n-1-|m_\ell|)$ to $(n-1-|m_\ell|)$ in steps of 2. If an H atom is excited to a state the energy of which is lowered in an electric field ('red-shifted' or 'high-field seeking' state) it decelerates as it flies out of this field, whereas an atom excited to a blue-shifted, low-field seeking state accelerates. The loss/gain in kinetic energy is equal to $\Delta E = \frac{3}{2}nk\Delta F$.

2. Experimental procedure

The experimental set-up is displayed schematically in figure 1 and consists of a source of H atoms in a supersonic beam [20], a laser system to excite them to Rydberg states and a Rydberg Stark decelerator [15].

To generate a supersonic beam containing H atoms, a 10:1 Ar:NH_3 gas mixture is pulsed out of a solenoid valve (repetition rate 10 Hz, stagnation pressure 3 bar, pulse length 250 μs). Before expanding into the vacuum, the beam passes through a 1 mm diameter quartz capillary where the H atoms are formed by the 193 nm photolysis of NH_3. After collimation

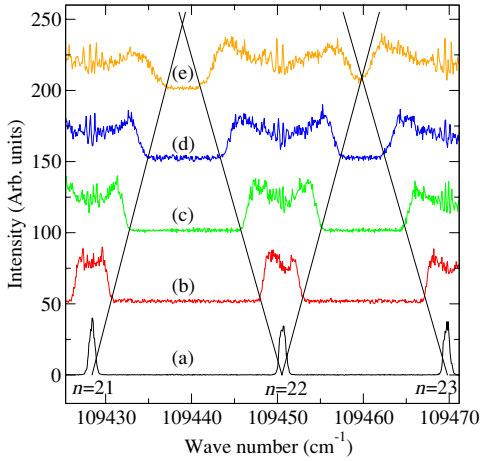

Figure 2. Stark spectra of atomic hydrogen recorded following two-photon excitation via the $n = 2\,^2$P state. The traces correspond to experiments in which the atoms were excited in the inhomogeneous field region of the decelerator. Potentials of ±0 V (a), ±25 V (b), ±50 V (c), ±75 V (d) and ±100 V (e) were applied to the first two plates of the decelerator, the two plates on the detector side being maintained at 0 V.

with a 0.5 mm diameter skimmer 2 cm downstream from the capillary exit, the gas beam is intersected at right angles by the counterpropagating VUV and UV laser beams used to excite the H atoms to Rydberg states via the $n = 2\,^2$P state in the middle of the four electrodes of the Stark decelerator. VUV radiation at Lyman α is generated by resonance-enhanced difference-frequency mixing in a cell filled with ∼10 mbar krypton. The doubled output of another Nd:YAG-pumped dye laser is used to excite the H atoms from the $n = 2\,^2$P state to Rydberg states. After photoexcitation, the Rydberg atoms continue their trajectories in the inhomogeneous field of the decelerator and are accelerated or decelerated depending on whether they were excited to a low- or a high-field seeking Stark state.

The inhomogeneous electric field was generated by applying constant voltages of opposite sign to the two electrodes separated by 6 mm on the nozzle side of the decelerator and keeping the two electrodes on the detector side at 0 V. The atoms thus moved from a high-field region towards zero field and consequently the Stark states with $k > 0$ ($k < 0$) were subject to an accelerating (decelerating) force. After leaving the decelerator, the Rydberg atoms traverse a 20 cm long field-free region before they ionize at a microchannel plate detector where their time of flight (TOF) is registered. The pressure in the decelerator rises from a background value of 10^{-7} mbar to 3×10^{-7} mbar during the experiments.

For the deceleration experiments, photoexcitation was carried out in the inhomogeneous field region of the decelerator at the end of the first two electrodes. To maximize the photoionization cross section to the outer members of the manifold of Stark states, the polarization vectors of the VUV and UV beams were both chosen to lie parallel to the direction of the electric field vector [21]. The inhomogeneous nature of the field manifests itself as a strong inhomogeneous broadening of the outer Stark states visible in traces (b)–(e) in figure 2, which were recorded by applying voltages of ±25 V, ±50 V, ±75 V and ±100 V to the first electrodes. Only the central components of the Stark manifold with $|k| \approx 0$ appear sharp in these spectra because their energy is nearly field independent and the inhomogeneous line broadening is small. The voltages were immediately turned off after photoexcitation because, when they were maintained, the deceleration/acceleration of the Rydberg atoms was

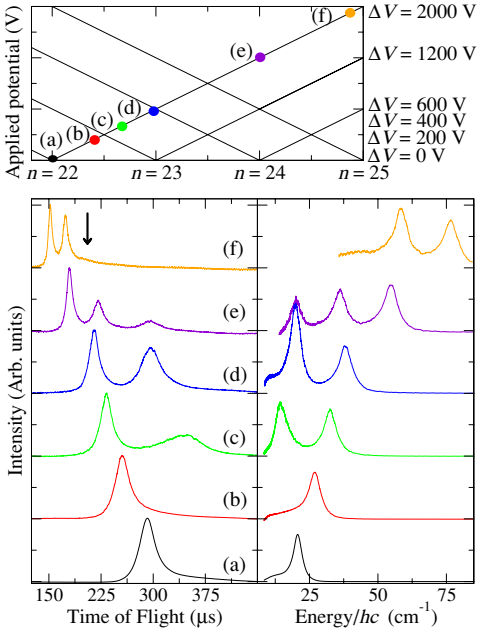

Figure 3. Upper panel: schematic map of the Stark states of H in the range of principal quantum number $n = 22$–25. The dots in this panel correspond to the positions where the acceleration/deceleration experiments shown in the lower panel were performed. Lower left panel: TOF spectra of the H atoms recorded at the positions indicated in the top panel. Lower right panel: kinetic energy distribution extracted from the experimental TOF spectra.

so strong, and the changes in the times of flight so large, that the measurement of reliable relative intensities for the different Stark states was impossible. The almost linear nature of the Stark effect is indicated by the diagonal lines in figure 2.

3. Results

Figure 3 summarizes a set of TOF measurements of the Rydberg atoms carried out after photoexcitation to the blue-shifted Stark states of $n = 22$ at several fields, which are indicated as dots in the schematic Stark map displayed in the upper panel. The bottom trace (trace (a)) in the lower panels corresponds to the zero-field reference measurement. The initial velocity determined from this measurement is 702(10) m s^{-1} and the relative longitudinal velocity distribution corresponds to a temperature of 0.1 K. The H atoms in the beam thus have a kinetic energy $E_{\rm kin}/hc = 20.8$ cm^{-1} when they enter the decelerator. At an applied voltage of ± 100 V (trace (b)), the times of flight are shifted by ≈ 50 μs to earlier times as expected for a low-field seeking state. The peak in the distribution corresponds to a final kinetic energy of $E_{\rm kin}/hc = 27.1$ cm^{-1}. At ± 200 V, above the Inglis–Teller field at $n = 22$ (trace (c)), the outer red-shifted Stark states of the $n = 23$ manifold are also excited by the laser because the strongly inhomogeneously broadened lines overlap. The atoms in the red-shifted states are decelerated and their times of flight increase by about 60 μs, corresponding to a final kinetic energy of $E_{\rm kin}/hc = 14.6$ cm^{-1}, whereas the atoms in the blue-shifted Stark states are accelerated to a final kinetic energy of $E_{\rm kin}/hc = 32.7$ cm^{-1}. The late peak in the TOF spectrum (c) not only shows how efficiently atoms can be decelerated but also illustrates the problems that arise when detecting the atoms that are slowed down to close to zero velocity:

the TOF distribution becomes very broad and rapidly shifts towards long times of flight so that very slow atoms can no longer be detected in TOF measurements. The TOF spectrum recorded at ±300 V shows two peaks at final kinetic energies of 38.2 and 20.1 cm^{-1}, corresponding to a blue-shifted Stark state with $n = 22$ and a $k \approx 0$ state of $n = 23$, respectively. The position of the latter of these two TOF peaks is almost the same as for the reference measurement, as expected for $k \approx 0$ states. At an applied voltage of ±600 V, the blue Stark states of the $n = 22$ manifold overlap spectrally with less blue-shifted Stark states with $n = 23$ and with $n = 24$, $k \approx 0$ Stark states. Consequently, three peaks are observed in the TOF spectrum at positions corresponding to final kinetic energies of 55 cm^{-1}, 36.2 cm^{-1} and 20.3 cm^{-1} for the Stark states with $n = 22$, 23 and 24, respectively. The top trace (f) in figure 3 represents a measurement recorded at ±1000 V, above the field-free position of the $n = 25$ states. Here, only two maxima are observed in the TOF spectra corresponding to the acceleration of the blue-shifted states with $n = 22$ and $n = 23$ to final kinetic energies of 76.7 cm^{-1} and 58.5 cm^{-1}, respectively. At the corresponding field strength of more than 3000 V cm^{-1}, the $n \geqslant 24$ Stark states within the laser bandwidth are all field ionized and do not contribute to the TOF spectrum.

Had some of the crossings between the blue-shifted Stark states of $n = 22$ and red-shifted states of $n = 24$ not been traversed diabatically at fields below their ionization field, a third peak would have been observed at the position indicated by an arrow above trace (f). The absence of any signal at this position can thus be interpreted as the (expected) diabatic traversal of the crossings between the Stark states [22]. Given that ≈10 such crossings are traversed that could potentially have led to a signal at $n = 24$, the absence of any detected signal enables one to set an upper limit to the probability of an adiabatic traversal of any given crossing. At the sensitivity of the present experiment (the two early TOF peaks in trace (f) have a signal-to-noise ratio of ≈100) we find this upper limit to be 0.1% at an electric field slew rate of 6×10^8 V cm^{-1} s^{-1}. In our previous experiments on argon, this probability was found to be unity. The qualitatively different behaviour of the Stark states of H atoms in time-independent fields compared with other atoms, which also results in their different field ionization dynamics [22], can thus be fully exploited to optimize the deceleration of H.

Converting the TOF scale in the lower left-hand-side panel of figure 3 into a kinetic energy scale (see lower right-hand-side panel of figure 3) demonstrates that the Rydberg atoms can be as efficiently decelerated as they can be accelerated. Indeed, the two peaks in trace (c) have the same integrated intensity. Unfortunately, the stopping of the Rydberg atoms cannot be demonstrated directly in our present experimental configuration because stopped atoms cannot reach the detector. However, the acceleration measurements indirectly prove that stopping the Rydberg atoms is feasible.

4. Discussion and conclusions

Table 1 summarizes the results of the quantitative analysis of the TOF spectra shown in figure 3 and compares the measured changes in kinetic energy with the Stark shift. Although the Stark shift is difficult to extract for any given Stark state because of the inhomogeneity of the electric field, it can be accurately determined by taking the difference between the calibrated laser excitation energy and the known zero-field energy levels of the H atom. The following conclusions can be drawn from the results summarized in figure 3 and table 1.

(1) The observed kinetic energy changes are equal to the Stark energies within the uncertainty of the measurement, and no changes in the quantum numbers of the initially prepared Stark states can be detected during the 3–6 μs long traversal of the deceleration stage.

Table 1. Summary of acceleration/deceleration experiments on $n = 22, k = 21$ H atoms in time-independent fields. The Stark shift was calculated as the difference between the laser excitation energy and the zero-field position of the Rydberg states. The change in kinetic energy $\Delta E_{\rm kin}$ was determined from the maxima of the energy distributions.

Applied voltage (V)	n	Stark shift ($\rm cm^{-1}$)	$\Delta E_{\rm kin}/hc$ ($\rm cm^{-1}$)
0		0	0
±100	22	6.4	6.3
±200	22	12	11.9
	23	−7	−6.2
±300	22	18.6	17.4
	23	−1.4	−0.7
±600	22	34.5	34.2
	23	15.6	15.4
	24	−1.5	−0.5
±1000	22	57	55.9
	23	38.1	37.7
	24	21.1	–

This conclusion was verified independently by selective field ionization. Consequently, beams of H atoms in selected Stark states with freely adjustable kinetic energy can be produced that could be used in scattering experiments.

(2) Changes of kinetic energy of up to three times the initial kinetic energy of the H atoms can be readily achieved. This observation directly implies that H atoms can be stopped using our 3 mm long decelerator provided that their initial kinetic energy is less than $E_{\rm kin}/hc = 55\ \rm cm^{-1}$ (or $E_{\rm kin} = 1.1 \times 10^{-21}$ J, corresponding to an initial velocity of $1150\ \rm m\ s^{-1}$). This very large improvement over previous experiments in which the initial kinetic energy could only be modified by a few per cent [11–13, 15, 23] results from the small mass of the H atoms and from the fact that the crossings of the Stark states are traversed diabatically which enables one to use electric fields several times larger than the Inglis–Teller field.

(3) Upper bounds of 0.1% for the probability of adiabatic traversals of the crossings between Stark states at a slew rate of $6 \times 10^8\ \rm V\ cm^{-1}\ s^{-1}$ and of $2.5 \times 10^{-4}\ \rm cm^{-1}$ for the magnitude of the avoided crossing at $n = 22$ were derived. In our experiments on argon, this probability was found to be 100%.

(4) The average acceleration over the length of the decelerator can be as high as $2 \times 10^8\ \rm m\ s^{-2}$. By expressing the acceleration in terms of the average field gradient ∇F, the mass m of the decelerated particle and the quantum numbers n and k of the Stark state

$$a(\rm m\,s^{-2}) = 76\,\nabla F(\rm V\ cm^{-2})\frac{1}{m(u)}nk, \tag{2}$$

one sees that a field gradient of only $350\ \mu\rm V\ cm^{-2}$ is sufficient to accelerate a hydrogen (or an antihydrogen) atom in a blue- or red-shifted Stark state with $n \geqslant 20$ as efficiently as the earth gravitational field. Potential future experiments to determine the sign of the gravitational force on antihydrogen atoms may thus have to consider the effects of the gradients of possible stray electric fields if such experiments are to be carried out on the excited antihydrogen atoms that are currently being produced at CERN [17, 18].

(5) Two-dimensional electrostatic trapping following the deceleration of the H atoms in high-field seeking states is within reach but necessitates several modifications associated with

the operation of the deceleration stage with time-dependent fields and the introduction of a field ionization method to detect the stopped Rydberg atoms. This work is currently underway in our laboratory.

Acknowledgments

We thank H Schmutz for his help in the realization of the detection system and Dr S Willitsch (Oxford) for his contribution to the development of the H-atom source. This work is supported by the Swiss National Science Foundation and the ETH-Zürich under project no TH-28/02-3.

References

[1] Bethlem H L and Meijer G 2003 *Int. Rev. Phys. Chem.* **22** 73
[2] Doyle J, Friedrich B, Krems R V and Masnou-Seeuws F 2004 *Eur. Phys. J.* D **31** 149
[3] Mourachko I, Li W and Gallagher T F 2004 *Phys. Rev.* A **70** 031401
[4] Lukin M D *et al* 2001 *Phys. Rev. Lett.* **87** 037901
[5] Tong D *et al* 2004 *Phys. Rev. Lett.* **93** 063001
[6] Gallagher T F, Pillet P, Robinson M P, Laburthe-Tolra B and Noel M W 2003 *J. Opt. Soc. Am.* B **20** 1091
[7] Pohl T, Pattard T and Rost J M 2003 *Phys. Rev.* A **68** 010703
[8] Singer K, Reetz-Lamour M, Amthor T, Marcassa L G and Weidemüller M 2004 *Phys. Rev. Lett.* **93** 163001
[9] Afrousheh K *et al* 2004 *Phys. Rev. Lett.* **93** 233001
[10] Breeden T and Metcalf H 1981 *Phys. Rev. Lett.* **47** 1726
[11] Procter S R, Yamakita Y, Merkt F and Softley T P 2003 *Chem. Phys. Lett.* **374** 667
[12] Vliegen E, Wörner H J, Softley T P and Merkt F 2004 *Phys. Rev. Lett.* **92** 033005
[13] Yamakita Y, Procter S R, Goodgame A L, Softley T P and Merkt F 2004 *J. Chem. Phys.* **121** 1419
[14] Softley T P 2004 *Int. Rev. Phys. Chem.* **23** 1
[15] Vliegen E and Merkt F 2005 *J. Phys. B: At. Mol. Opt. Phys.* **38** 1623
[16] Vanhaecke N, Comparat D and Pillet P 2005 *J. Phys. B: At. Mol. Opt. Phys.* **38** S409
[17] Amoretti M *et al* 2002 *Nature* **419** 456
[18] Gabrielse G 2005 *Adv. At. Mol. Opt. Phys.* **50** 155
[19] Gerlach W and Stern O 1922 *Z. Phys.* **9** 349
[20] Willitsch S, Dyke J M and Merkt F 2003 *Helv. Chim. Acta* **86** 1152
[21] Delsart C, Cabaret L, Blondel C and Champeau R-J 1987 *J. Phys. B: At. Mol. Phys.* **20** 4699
[22] Gallagher T F 1994 *Rydberg Atoms* (Cambridge: Cambridge University Press)
[23] Vliegen E, Limacher P A and Merkt F 2006 *Eur. Phys. J.* D at press